# PROPWASH IMPACTS ON WATER QUALITY AROUND DREDGING AND OTHER MARINE CONSTRUCTION ACTIVITIES

Donald F. Hayes[1], Rohit Chintamaneni[2], Prathyusha Bommareddy[2], and Bhaskar Cherukuri[2]

## ABSTRACT

Propeller-induced sediment resuspension has been raised as a concern around dredging and other marine construction activities on many projects. Some measurements of sediment resuspension due to large vessel movement have been gathered and reported. These indicate the rate of sediment resuspension is potentially significant. Several models have also been developed that look at propeller-induced erosion. This paper takes the most applicable of these scour models and applies it to vessels commonly used in dredging and other marine construction activities. Sediment resuspension rates are presented for a range of operating conditions for each vessel.

**Keywords:** Dredging, water quality, sediment resuspension, prop wash, water quality modeling

## INTRODUCTION

Propeller and wake induced shear stresses from waterborne vessels often exceed the critical shear stress[3] of the bottom sediments, resuspending them into the water column. The *critical shear stress* in this context refers to the shear stress required to initiate motion of sediment grains currently at rest (i.e. erosion) at the sediment-water interface. Figure 1 shows clearly visible turbidity plumes from a tug and cargo ship in a deep-draft channel (authorized depth of 45 ft). Support vessel operations associated with marine construction, including dredging, also represent potentially significant sources of sediment resuspension. Since these support vessels often work in shallow water with soft sediment bottoms, the sediment resuspension potential resulting from their movement is significant.

**Figure 1. Turbidity plumes from a tug with tow and a cargo vessel in a deep draft navigation channel.**

A number of studies have evaluated sediment resuspension associated with marine vessel movement (Johnson, 1976; Erdmann et al, 1994; Pettibonea et al, 1996; Ravens and Thomas, 2008). Many of these studies collected site-specific data and their results can only be extrapolated in the most general sense to other sites. Several researchers, however, have developed bottom velocity and shear stress models that apply to a broad range of vessels (Verhey, 1983; Hamill et al., 1999; and Maynord, 2000). Combined with site-specific sediment erosion versus shear stress data, these models can provide reproducible estimates of bottom sediment erosion under specific operating conditions. This paper combines these results and computes sediment resuspension rates for vessels representative of those used in dredging and other marine construction operations.

## PROP WASH MODELS

The earliest study on water quality impacts resulting from marine traffic identified was by Johnson (1976). This study evaluated the effects of tow traffic on sediment resuspension and water quality in the Upper Mississippi and

[1]Director, Institute for Coastal Ecology and Engineering and Professor, Department of Civil Engineering, University of Louisiana at Lafayette, P.O. Box 42291, Lafayette, LA 70504-229; Phone: 337/482-5929, FAX: 337/482-6688, hayes@louisiana.edu.
[2]Graduate Research Assistant, Institute for Coastal Ecology and Engineering, Department of Civil Engineering, University of Louisiana at Lafayette, P.O. Box 42291, Lafayette, LA 70504-229.

Illinois Rivers. A number of additional studies have been conducted since that time such as those by Erdmann et al (1994), Pettibonea et al (1996), and even as recently as Ravens and Thomas (2008). All of these studies add credence to the concern over vessel-induced sediment resuspension and provide useful data on site-specific observations. They do not, however, provide sufficient information to generate sediment resuspension flux rates over a range of vessels and conditions. However, three models were identified in the literature that are capable of estimating the propeller-induced sediment scour. These models are described in Verhey (1983), Hamill et al. (1999), and Maynord (2000). While the models have similar purposes, capabilities are rather different. The equations in the models are similar, however, and originate from the work done by Albertson et al. (1948).

Verhey's model was the first attempt to model prop-induced scour found in the literature. Unfortunately, it applies only to large stone sizes (~ 0.1 m to 0.3 m) (Verhey 1983). Hamill's model calculates maximum scour and its location relative to the propeller. The model applies only to non-cohesive sediments and assumes vertical homogeneity. It is also limited to applications where the depth from the maximum draft (propeller tip) to the sediment is between 50% and 250% of the propeller diameter. Since the water quality concerns that are the focus of this paper revolve around fine sediments, neither of these models are applicable.

Fortunately, Maynord (2000) presented a combination of models that provide maximum velocity estimates at locations along the sediment-water interface. It considers important physical characteristics of the vessel including length, width, draft, propeller size and depth, and propeller spacing for dual engines. Vessel movement is also an important variable, so the model considers both forward speed and applied horsepower. The primary environmental characteristic of importance is water depth.

**Maynord Model Description**

Maynord (2000) presented 2 models to compute maximum bottom velocities at specific locations relative to the propeller position resulting from boat movement and propeller action. The models consider physical site conditions and vessel characteristics and operation. The model for Zone 1 predicts velocities within a distance of 10 propeller diameters. The Zone 2 model predicts velocities beyond that distance. The equations comprising Maynord's models are:

**Zone 1 Model: Applies to distances less than 10 propeller diameters behind the propeller ($X_p < 10\ D_p$)**

$$V_1(X_p, Y_{cl}) = AX_P^{-0.524}\left(e^{\frac{-15.4R_1^2}{X_P^2}} + e^{\frac{-15.4R_1^2}{X_P^2}}\right) \quad (1)$$

where:

$$A = 1.45V_2D_p^{0.524} \quad (2)$$

$$R_1^2 = \left(Y_{cl} - 0.5W_p\right)^2 + \left(H_p - C_j\right)^2 \quad (3)$$

$$R_2^2 = \left(Y_{cl} + 0.5W_p\right)^2 + \left(H_p - C_j\right)^2 \quad (4)$$

$$C_j = -\left[0.213 - 1.05\left(\frac{C_p g}{V_2^2}\right)\left(X_p - 0.5L_{set}\right)\right]\left(X_p - 0.5L_{set}\right) \quad (5)$$

$$V_2 = \frac{1.13}{D_0}\sqrt{\frac{T}{\rho_w}} \quad (6)$$

$$C_p = 0.12\left(\frac{D_p}{H_p}\right)^{0.67} \quad \text{(kort nozzle propeller; } C_p = 0.04\text{)} \quad (7)$$

$$EP = 23.57P_{hp}^{0.974} - 2.3V_w^2P_{hp}^{0.5} \quad \text{(kort nozzle propeller; } EP = 31.82P_{hp}^{0.974} - 5.4V_w^2P_{hp}^{0.5}\text{)} \quad (8)$$

$$D_0 = 0.71D_p \qquad \text{(kort nozzle propeller; } D_0 = D_p\text{)} \quad (9)$$

**Zone 2 Model: Applies to distances greater than 10 propeller diameters behind the propeller ($X_p > 10D_p$)**

$$^{Z2}V(X_p, Y_{cl}) = 0.34 V_2 C_1 \left(\frac{D_p}{H_p}\right)^{0.93} \left(\frac{X_p}{D_p}\right)^{0.24} e^{-\left(\frac{0.0178 X_p}{D_p} + \frac{Y_{cl}^2}{2C_{Z2}^2 X_p^2}\right)} \quad (10)$$

where:

$$C_{Z\,2} = 0.84\,(X_p/D_p)^{-0.62} \quad (11)$$

$$C_1 = 0.66 \text{ (for Kort nozzle propeller; } C_1 = 0.85) \quad (12)$$

and,

$X_p$= Distance behind the propeller, m
$D_p$= Propeller diameter, m
$W_p$= Distance between propeller, m
$L_{set}$= Distance from ship stern to propeller, m
$H_p$ = Distance from center of propeller axis to channel bottom, m
$Y_{cl}$ = Lateral distance from ship centerline, m
$C_j$ = Vertical distance from propeller shaft to location of maximum velocity within the jet, m
$\delta_p$ = Propeller depth, m
g = acceleration of gravity, $m/s^2$
$C_p$= Propeller coefficient, dimensionless
T = Forward Thrust, N
$\rho_w$=Density of water, $kg/m^3$

The variable $X_p$ represents the distance behind the propeller while $Y_{cl}$ represents the lateral position relative to the boat centerline. Since many marine vessels have multiple engines and propellers, the model accounts for the interaction and eventual combination of the individual jets. Zone 1 is the region behind the vessel where each propeller jet acts independent and produces a separate velocity field. In areas where the bottom velocity distributions from the two propeller streams overlap, total bottom velocity is determined by superposition of the velocity distributions. Zone 2 begins after the velocity fields merge into a single velocity distribution, estimated to be about 10 propeller diameters behind the propellers. The primary concern is that transitions between Zone 1 and Zone 2 can sometimes be abrupt and, therefore, unrealistic since one would typically expect gradual velocity variations.

The bottom shear stress resulting from these velocities can be compared to the critical shear stress of the sediment to determine erosion potential. Shear stress experienced by the sediment surface due to this velocity is calculated as:

$$\tau = 0.5 \rho_w C_{fs} V^2_{prop} \quad (13)$$

where,

$$C_{fs} = 0.01\left(\frac{D_p}{H_p}\right) \quad (14)$$

and,

$C_{fs}$ = bottom friction factor for propeller wash, dimensionless
$\tau$ = bottom shear stress, $N/m^2$
$V_{prop}$ = bottom velocity due to propeller wash, m/s
$\rho_w$= water density, $kg/m^3$

A sediment-specific relationship between shear stress and erosion rate is used to allow the model to be applied to any sediment, regardless of grain sizes or other sediment characteristics. Impending motion of the sediment grains begins at the critical shear stress and erosion rate increases with increasing shear stress. The relationship between erosion rate versus shear stress is typically assumed to be:

$$\varepsilon = 0 \qquad \text{for } \tau < \tau_{cr} \quad (15)$$

$$\varepsilon = a\tau^n \qquad \text{for } \tau \geq \tau_{cr} \tag{15}$$

where,

ε = volumetric sediment erosion rate, m/sec
$\tau_{cr}$ = critical shear stress, Pa
a = regression coefficient, m/sec/Pa
n = regression coefficient, dimensionless

Gailani (2001) showed that it is also possible to fit data for moderate shear stresses (< 1.5 Pa) to the equation:

$$\varepsilon = a\left(\frac{\tau - \tau_{cr}}{\tau_{cr}}\right)^n \tag{16}$$

The regression parameters a and *n* are sediment specific and typically developed from laboratory studies. The values of these regression parameters typically vary with depth as sediment characteristics change.

Several approaches have been developed to determine the shear stress-sediment scour relationship. SEDFLUME testing is probably the most commonly used of these approaches. The SEDFLUME allows a sediment core to be subjected to a range of flow-induced shear stress to determine erosion rates. The results are used to determine the regression coefficients A and n. Additional information on SEDFLUME testing can be found in McNeil et al. (1996).

## SEDIMENT FLUX MODEL

Maynord's model combined with a shear stress-erosion rate relationship provides useful information on the potential erosion that might result from specific vessel operations. These can also be used to develop sediment flux estimates from a moving vessel by modifying the bathymetry based upon the computed erosion rates and reapplying the model to develop new erosion rates. That approach is described below.

The basis of the model is a river, channel, or estuarine area covered by a discretized grid in the X-Y (horizontal) plane. The depth of each cell in the grid is defined as $Z_{ij}$. While grid cell size is not important to the mathematical formulation, it must be sufficiently small to adequately describe bottom velocity variations produced by the model above. A cell of 1 m x 1 m is probably adequate, although smaller cells provide more accurate results.

Applying Maynord's model to a specific vessel located within the surface grid provides maximum bottom velocities relative to the vessel location. Note that these velocities are relative to the propeller location. Positive $X_p$ values in the equations shown in Figure 2 are in the opposite direction of the vessel's forward movement, i.e. if the vessel is moving forward at 1 knot along a 135° vector (notice that these are relative to the X-Y grid, not North), positive $X_p$ values would increase along a 315° vector. $Y_{cl}$ values are normal to the vessel's longitudinal centerline; in the example above, positive values would extend along a 45° vector from the propeller position while negative values extended along a 225° vector. The relationship between any node in the X–Y grid and the $X_p$-$Y_{cl}$ grid for a propeller position of $X_o$,$Y_o$ is:

$$X_p = L\cos(\beta) \tag{17}$$

$$Y_{cl} = L\sin(\beta) \tag{18}$$

where

$$L = \sqrt{(X - X_o)^2 + (Y - Y_o)^2} \tag{18}$$

$$\beta = -\alpha + tan^{-1}\left(\frac{(Y - Y_o)}{(X - X_o)}\right) \tag{19}$$

α = angle from thrust direction to X-axis, degrees

Figure 2 illustrates the grid overlays for a vessel moving along a 315° vector.

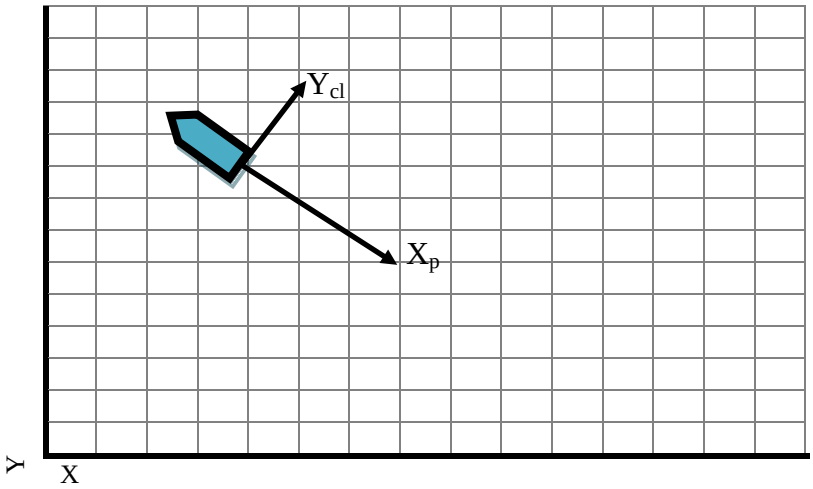


**Figure 2. Example grid overlays for flux computations.**

Maynord's models can be used to estimate the maximum bottom velocity at each node. All of the model parameters remain the same for all nodes except depth from propeller centerline to the sediment surface which reflects localize bathymetry. That depth can be computed at each node as:

$$(H_p)_{ij} = Z_{ij} - \delta_p \tag{21}$$

where,

$(H_p)_{ij}$ = depth from propeller centerline to the sediment surface at node i,j, m
$Z_{ij}$ = total water depth at node i,j, m

Fed these values of $(H_p)_{ij}$, the models provide maximum bottom velocities for each node in the positive $X_p$ domain; velocity values are zero for all negative values of $X_p$.

Utilizing Maynord's models in this manner has two potential flaws. First, the models were developed for relatively smooth bathymetry and do not check continuity between locations. Fortunately, the resulting error should be relatively small unless large, abrupt bathymetric variations exist. The second flaw is the inconsistent transition between Zone 1 and Zone 2 velocities. In some cases, Zone 1 velocities are less than Zone 2 velocities for values of $X_p$ less than $10D_p$, resulting in an abrupt velocity increase at $X_p = 10D_p$. Such an abrupt velocity increase will not occur and is the result of model formulation. These discontinuities were addressed in this application by substituting the initial Zone 2 velocity at $10D_p$ for any lower velocities along a constant $Y_{cl}$ line. This forced a smooth transition between the zones. This approach does result in higher velocities within Zone 1 than computed by the Zone 1 models. The discontinuities, however, occurred primarily along the fringes of the propeller-induced velocity field in areas of low velocity and tended not to significantly impact the computed scour volume.

Maximum bottom velocities at each node can be translated into sediment erosion rate using the relationships provided above. Except in the most extreme cases – which are not likely realistic - most of the grid will experience shear stresses less than the critical shear stress, indicating no bottom sediment erosion will occur. The zone of highest velocities and, subsequently, erosion is usually limited to an oval-shaped area slightly off-set from the centerline of each propeller. Figure 3 shows an example of these high velocity areas behind a twin-propeller tug.

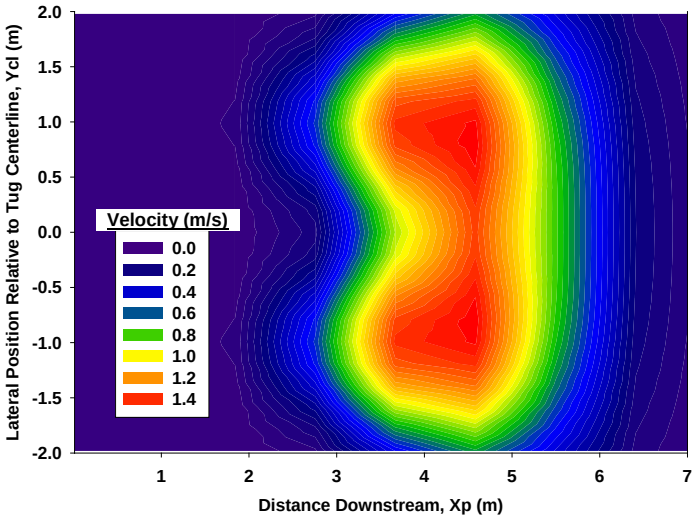


**Figure 3. Maximum sediment surface velocities behind a large tug (P = 900 HP; $H_d$ = 2.7 m).**

Bottom sediment erosion increases the water depth as it occurs; as the depth increases, local bottom velocities decrease and erosion decreases. Thus, the initial erosion rate is accurate only until erosion changes the bathymetry sufficiently to result in a measurable decrease in bottom velocity and erosion rate. Thus, the model must be continuously reapplied updated bathymetry to produce accurate results. As erosion occurs, bathymetric changes can be computed at each node as:

$$Z_{i,j}^{t+1} = Z_{i,j}^{t} + \varepsilon_{i,j}^{t} \Delta t \tag{22}$$

where the superscript t denotes specific time steps and

$\Delta t$ = time step increment, min

The suspended sediment flux during the time step can be computed as:

$$g^{t} = \sum_{j=1}^{n} \sum_{i=1}^{m} \varepsilon_{i,j}^{t} \Delta X \Delta Y \gamma_s \Delta t \tag{23}$$

where,

g = suspended sediment flux, kg/sec
$\Delta X$ = x-grid increment, m
$\Delta Y$ = y-grid increment, m
$\gamma_s$ = dry sediment density, kg/m$^3$

Except in unusual cases, the vessel will be moving – or attempting to move – forward. As the vessel moves, the propeller position and $X_p$-$Y_{cl}$ grid location (which is relative to the propeller position) continuously change, moving along opposite the direction of thrust. Thus, while the $X_p$-$Y_{cl}$ locations of the highest bottom velocities remain relatively constant, their positions in the X-Y grid continuously change with vessel movement. The resulting movement of the bottom shear stress distributions with vessel movement provides for a relatively accurate assessment of the resulting sediment resuspension.

## MODEL APPLICATION

### Site Characteristics

The models were applied to a simplified, hypothetical site to facilitate comparisons between vessels. The site was assumed to consist of a perfectly flat bathymetry extending infinitely in all directions. Water depths from 2 to 10 m were used to evaluate the affect of water depth on scour. The bottom sediment was assumed to be infinitely thick soft silty clay with an in situ water content of 62.5%, specific gravity of 2.75, and 0.53% organic content.

The following relationships between shear stress and erosion rate were developed from SEDFLUME test results:

$$\varepsilon = 0 \qquad \text{for } \tau < 1.21 \text{ Pa} \tag{24}$$

$$\varepsilon = 5.1089\left(\frac{\tau}{1.21} - 1\right)^{0.9182} \qquad \text{for } 1.52 \text{ Pa} \geq \tau \geq 1.21 \text{ Pa} \tag{25}$$

The rate at which erosion rates could be accurately measured in the SEDFLUME was exceeded at about 1.52 Pa. Since the prop-wash models may generate shear stresses in excess of 1.52 Pa, it was necessary to establish a relationship to extrapolate the results beyond the laboratory data. The power curve relationship above generates excessively large erosion rates at small increases in shear stress. The resulting extrapolation was thought to likely overestimate resuspension flux. Thus, the following linear relationship was used to extrapolate the results for shear stresses greater than 1.52 Pa:

$$\varepsilon = 1.46 + 24.8(\tau - 1.21) \qquad \text{for } \tau \geq 1.52 \text{ Pa} \tag{26}$$

This relationship was chosen because it should not produce excessive erosion rates, i.e. the resulting resuspension flux should not be overstated. This approach has not been proven to be accurate and this work should not be taken as proving its viability.

### Vessel Selection and Operation

Dredging and other marine construction operations use a wide range of vessels. A range of representative vessels was selected for comparison. Table 1 provides the physical characteristics of those vessels.

**Table 1. Representative vessels used in dredging and other marine construction activities. Note that all vessels have dual engines and propellers.**

| Vessel | Length (m) | Beam (m) | Draft (m) | Depth to Center of Prop Shaft (m) | Width Between Props (m) | Distance from Prop to Stern (m) | Total HP (both engines) | Prop Dia. (m) |
|---|---|---|---|---|---|---|---|---|
| 1800 HP Tug | 22.1 | 7.4 | 3.2 | 2.3 | 3.0 | 1.5 | 1800 | 1.8 |
| 600 HP Pushboat | 7.7 | 4.2 | 1.5 | 0.7 | 1.3 | 0.7 | 600 | 0.9 |
| 180 HP Pushboat | 7.6 | 3.1 | 0.6 | 0.6[a] | 1.0 | 0.7 | 180 | 0.4 |

[a]Depth to Center of Prop. Shaft is approximate because jack-plates can adjust prop depth.

### Computational Details

A uniform computational grid was used with 0.152 m cells in both the X and Y direction. Each vessel was allowed to move forward without turning over the bathymetry until a steady-state resuspension flux rate was achieved. The forward speed was varied from 1 to 10 knots while applied horsepower was varied from 0 to the maximum horsepower. Computations were made at 0.1 second time steps to minimize error when the computations produced excessive scour rates. Steady-state was reached within the first few minutes of movement in most cases.

## RESULTS

Table 2 summarizes approximate dimensions of the areas scoured and the steady-state suspended sediment fluxes computed for the vessels described in Table 1 and the hypothetical site conditions used. Most importantly, these results are based upon highly erodible sediment conditions of unlimited depth. The results follow expected patterns, suggesting that they are comparable, i.e. the trends shown are likely accurate even if the computed flux values vary.

**Table 2. Predicted steady-state sediment resuspension flux from a range of vessels and operating conditions. All vessels are moving forward at 1 knot.**

| Applied Horsepower | Water Depth (m) | Prop Clearance (m) | Suspended Sediment Flux (kg/sec) | Scour Length (m) | Scour Width (m) |
|---|---|---|---|---|---|
| **1800 HP Tug** | | | | | |
| 450 | 4.0 | 1.7 | 13893 | 25.9 | 5.9 |
| 450 | 6.0 | 3.7 | 12464 | 20.1 | 6.9 |
| 450 | 8.0 | 5.7 | 10360 | 17.7 | 7.2 |
| 450 | 10.0 | 7.7 | 8279 | 15.2 | 7.5 |
| **600 HP Pushboat** | | | | | |
| 150 | 2.0 | 1.3 | 4294 | 21.6 | 4.1 |
| 150 | 4.0 | 3.3 | 3557 | 15.4 | 5.3 |
| 300 | 4.0 | 3.3 | 7989 | 30.2 | 8.7 |
| 150 | 6.0 | 5.3 | 1944 | 11.1 | 5.6 |
| 300 | 6.0 | 5.3 | 5302 | 24.1 | 9.6 |
| 150 | 8.0 | 7.3 | 536 | 6.5 | 5.0 |
| 300 | 8.0 | 7.3 | 2619 | 17.7 | 9.0 |
| 150 | 10.0 | 9.3 | 10 | 2.1 | 2.3 |
| 300 | 10.0 | 9.3 | 556 | 10.7 | 7.2 |
| **180 HP Pushboat** | | | | | |
| 45 | 2.0 | 1.4 | 998 | 16.3 | 5.6 |
| 90 | 2.0 | 1.4 | 2345 | 31.1 | 10.2 |
| 135 | 2.0 | 1.4 | 3505 | 43.6 | 12.4 |
| 180 | 2.0 | 1.4 | 5119 | 56.7 | 18.4 |
| 90 | 4.0 | 3.4 | 0 | 0.0 | 0.0 |
| 135 | 4.0 | 3.4 | 71 | 13.3 | 5.0 |
| 180 | 4.0 | 3.4 | 220 | 21.8 | 8.1 |

The results show that an 1800 HP tug operating at 25% power and moving forward at 1 knot over a range of depths could potentially resuspend almost 14,000 kg/sec at 4.0 m water depth to 8,300 kg/sec at 10.0 m water depth. A 600 HP pushboat operating similarly (25% power) could potentially resuspend 4,300 kg/sec at 2.0 m water depth, but that drops to 10 kg/sec at 10.0 m. Finally, a small pushboat (180 HP) could potentially resuspend 1000 kg/sec to 5000 kg/sec at 2.0 m water depth depending upon the power applied. However, the resuspension rates are much less at a depth of 4.0 m, requiring 75% power to achieve 70 kg/sec.

## DISCUSSION

The values of resuspension flux produced by the models for the example vessels are very high. For comparison, Table 3 shows resuspension rates that might be associated with dredging the same sediment. The results assume a perfectly efficient dredging operation with a one minute cycle time and 1% loss rate. The results show suspended sediment flux from dredging to be less than 5 kg/sec for bucket volumes up to 30 $m^3$, substantially less than most of the values shown for the vessels.

**Table 3. Sediment resuspension rates for a perfectly efficient bucket dredge with a 1 minute cycle time and 1 percent loss rate.**

| Sediment Volume per Bucket Cycle ($m^3$) | 5 | 10 | 15 | 20 | 25 | 30 |
|---|---|---|---|---|---|---|
| Resuspended Sediment Flux Rate (kg/sec) | 0.8 | 1.6 | 2.5 | 3.3 | 4.1 | 4.9 |

The significantly larger resuspended sediment flux rates predicted for vessel movement is quite surprising. Partially, they reflect the highly erodible nature of the sediment used in the computations. The erodability of these sediments is not unusual compared to many soft bottom sediments, although many sediments are substantially less erodable. However, the assumption of consistent erodability with depth is not applicable to most sites. Thus, these rates would not be sustained for extended periods. Lastly, the models do not consider transport and redeposition of sediment. It is likely that much of the eroded sediment would redeposit within a few meters of its point of erosion, particularly given the extensive erosion rates that would likely lead to sediment behavior as a mass rather than a suspension.

These reasons combined with the uncertainty and simplifying assumptions associated with the modeling approach advocate caution in placing too much emphasis on the actual numerical results shown in Table 2. However, the results suggest that high shear stresses can be induced by vessel traffic and those shear stresses pose significant potential for sediment resuspension. The results show that sediment resuspension is particularly a concern in shallow water. This suggests that care to minimize vessel traffic in shallow water areas would be appropriate to manage water quality impacts associated with marine construction operations. However, the results also seem to show that it is not possible to dredge enough to eliminate the problem.

In conclusion, the comparison of the results to dredging suggests that vessel traffic could contribute a similar amount of sediment resuspension – if not more – as dredging. A more extensive site specific study would be necessary to fully evaluate potential losses for any individual project.

## ACKNOWLEDGEMENTS

The authors would like to thank Alexandra Stroescu, Mahdi Mahmoudi, and Maryam Shafiee for their significant contributions to this paper. All are former graduate research assistants in Institute for Coastal Ecology and Engineering.

## REFERENCES

Albertson, M.L. 1948. Diffusion of Submerged Jets," *Proc. ASCE Transactions*, Paper no. 2409, pp. 639-664.

Erdmann, J.B.; Stefan, H.G.; Brezonik, P.L. 1994. "Analysis of Wind- And Ship-Induced Sediment Resuspension in Duluth-Superior Harbor," *Journal of the American Water Resources Association*, Volume 30 Issue 6, Pages 1043 – 1053.

Gailani, J. Z., Kiehl, A., McNeil, J., Jin, L. and Lick, W. (2001). "Erosion Rates and Bulk Properties of Dredged Sediments from Mobile, Alabama," *DOER Technical Notes Collection (ERDC TN-DOER-N10)*, U.S. Army Engineer Research and Development Center, Vicksburg, MS.

Hamill, G. A.; Johnston, H. T.; and Stewart, D. P. 1999. "Propeller Wash Scour Near Quay Walls," *Journal Of Waterway, Port, Coastal, And Ocean Engineering*, American Society of Civil Engineers, July/August 1999.

Hamill, G.A.; McGarvey, J.A.; and Hughes, D.A.B. 2004. "Determination of the Efflux Velocity from a Ship's Propeller," *Proceedings of the Institution of Civil Engineers, Maritime Engineering 157*, June 2004 Issue MA2, Pages 83-91.

Johnson, J.H. (1976). "Effects of Tow Traffic on the Resuspension of Sediments and on Dissolved Oxygen Concentrations in the Illinois and Upper Mississippi Rivers Under Normal Pool Conditions." *Technical Report Y-76-1*, Army Engineer Waterways Experiment Station, Engineering Effects Lab, Vicksburg.

Maynord, Stephen T. 2000. "Physical Forces Near Commercial Tows," *Interim Report*, U.S. Army Engineer Research and Development Center, Vicksburg, MS 39180-6199.

Maynord, Stephen T. 2004. "Ship Effects at the Bankline of Navigation Channels," *Proceedings of the Institution of Civil Engineers, Maritime Engineering* 157, June 2004, Issue MA2, Pages 93-100.

McNeil, J., Taylor, C., and Lick, W. (1996). "Measurements of Erosion of Undisturbed Bottom Sediments with Depth," *J. Hydr. Engrg.*, ASCE 122(6), 316-324.

Pettibonea, G.W.; Irvine, K.N.; Monahan, K.M. 1996. "Impact of a Ship Passage on Bacteria Levels and Suspended Sediment Characteristics in the Buffalo River, New York," *Water Research*, Volume 30, Issue 10, October 1996, Pages 2517-2521.

Ravens, T.M. and Thomas, R.C. 2008. "Ship Wave-Induced Sedimentation of a Tidal Creek in Galveston Bay," *J. Wtrwy., Port, Coast., and Oc. Engrg.*, Volume 134, Issue 1, pp. 21-29 (January/February 2008).

Verhey, B., 1983. "The Stability of Bottom and Banks Subjected to the Velocities in the Propeller Jet Behind Ships," *Proceedings of the 8th International Harbour Congress*, Antwerp Belgium, June 13-17, 1983.